CRBMseg: MRI Tissue Segmentation with a Continuous Restricted Boltzmann Machine

by
Andrew Kope

9840 Final Project
Department of Computer Science
University of Western Ontario
London, Ontario, CANADA
January, 2013

Course Instructor: Olga Veksler

Abstract

Existing brain magnetic resonance imaging (MRI) tissue segmentation algorithms, though approaching the performance of a manual expert segmentation, still leave room for performance improvements in both processing time and segmentation accuracy. The present paper describes a novel algorithm for automated brain MRI scan tissue segmentation which employs a continuous restricted Boltzmann machine, called CRBMseg. The results of a pilot performance test of CRBMseg are presented, and future refinements of the algorithm are discussed.

Keywords: automatic brain MRI tissue segmentation, restricted Boltzmann machine

CRBMseg: MRI Tissue Segmentation with a Continuous Restricted Boltzmann Machine

Segmentation of brain magnetic resonance imaging (MRI) volumes is the process of classifying each volume element (or voxel) into one of two or more distinct tissue types. Typically, brain MRI segmentation divides a volume into sections of white matter (WM), gray matter (GM), and cerebrospinal fluid (CSF). Brain MRI tissue segmentation has several applications, including building population atlases of brain tissue types, guiding surgeons in the operating room, and monitoring anatomical changes in the brain produced by medical treatments (Chung, Dinov, Toga & Vese, 2010).

Traditionally, brain MRI tissue segmentation has been performed manually by an expert with knowledge of brain anatomy. This is however very tedious and time consuming for the segmenter and, as such, manual segmentation is impractical for large data sets. Several automated approaches to brain MRI tissue segmentation have been proposed in the literature, most notably the FAST algorithm using a hidden Markov random field and the expectation maximization algorithm (Zhang, Brady & Smith, 2001), the SMP5-segment algorithm using a Gaussian probability model (Ashburner et al., 1995), and the FIRST algorithm using a Bayesian statistical model (Patenaude, Smith, Kennedy & Jenkinson, 2007). Although these methods all provide reasonable segmentations, none of them can provide the accuracy of manual expert segmentations. Given this performance gap, I present a novel method for brain MRI tissue segmentation employing a continuous restricted Boltzmann machine (CRBM) called CRBMseg.

Restricted Boltzmann Machines

A Continuous Restricted Boltzmann Machine is a stochastic neural network with two layers of continuous-valued nodes (or units), one layer visible to the observer and one hidden (Figure 1). Excluding bias nodes, the nodes of these two layers form a complete bipartite graph

(bias nodes are not connected to each other); with the exception of bias nodes, all of the network's connections are also bidirectional and symmetric (bias nodes do not receive activation from other nodes). Most notably, Boltzmann machines have been used to reduce the dimensionality of large data sets (e.g. Hinton & Salakhutdinov, 2006), have applications in signal processing (e.g. Mohamed & Hinton, 2010) and can be stacked to create so-called deep learning networks.

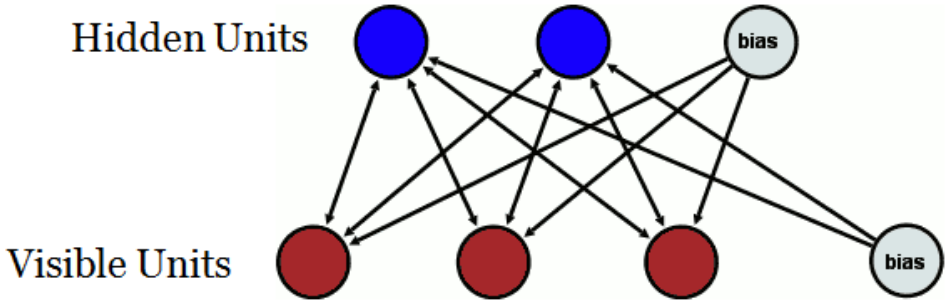

Figure 1. Restricted Boltzmann machine architecture, including bias nodes (imonad.com, 2013).

During training, the Contrastive Divergence algorithm (see Carreira-Perpinan & Hinton, 2004) is applied to iteratively change the weights of the network's connections. This change to the connections' weights encodes within the network the probabilistic distribution of visible layer states present in the training data. Once training is complete, the network is able to 'reconstruct' a maximally likely (or low energy) visible layer state from a novel input vector by iteratively spreading activation between the visible and hidden layers.

CRBMseg Pipeline

The CRBMseg algorithm uses a four step pipeline to perform the tissue segmentation of an input brain MRI scan (Figure 2). Given an input scan in the NIFTI (Neuroimaging Informatics Technology Initiative) data format, the brain is first isolated from the rest of the image using the FSL BET (FMRIB Software Library Brain Extraction Tool, Smith et al., 2004). Second, the bias

field of the scan is estimated and corrected for, again using the FSL BET. Following that correction, the intensity of the input scan is normalized to a reference scan using the Neuroimaging in Python (NiPy) histogram matching algorithm (see Gorgolewski et al., 2011). Finally, the scan is segmented into white matter, gray matter, and cerebrospinal fluid using a continuous restricted Boltzmann machine.

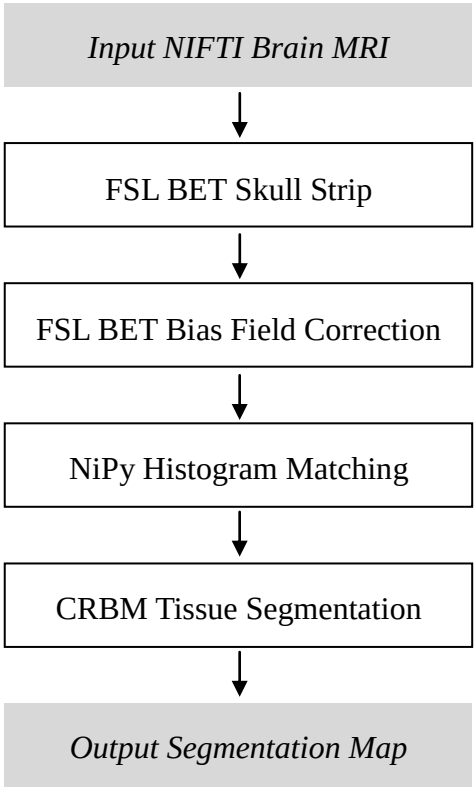

Figure 2. CRBMseg pipeline steps.

CRBM Tissue Segmentation

The CRBMseg algorithm uses a continuous restricted Boltzmann machine to discern the tissue type membership of each voxel of the preprocessed brain MRI scan. To accomplish this, the machine is first trained on a set of input vectors derived from a brain MRI scan which has already been manually segmented. Training vectors presently have 12 dimensions, corresponding

to: a given voxel's intensity in an MRI image, the intensities of its eight in-slice neighbours, and a three-digit binary code for the given voxel's tissue type (see Figure 3); voxel intensities are scaled from integers between 0 and 255 to decimals between 0 and 1. The length and specific parameters of training are specific to each implementation of the CRBMseg algorithm, however from a theoretical perspective the CRBM needs to be trained until it has accurately encoded the tissue code that corresponds to each voxel's (and its neighbours') intensity.

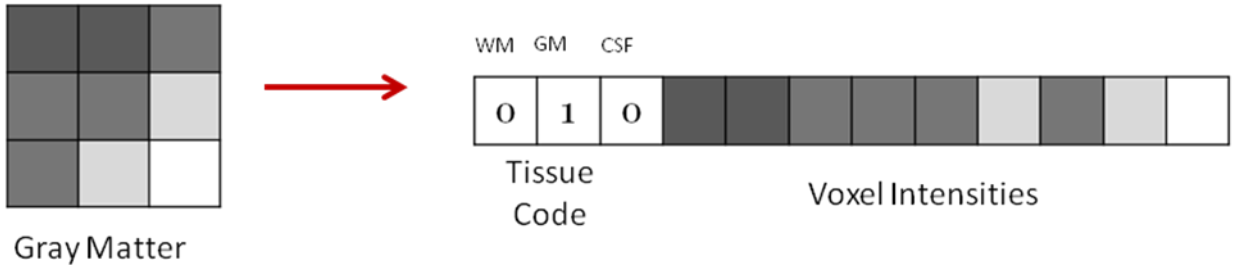

Figure 3. CRBM training input vector.

Once training is complete, the CRBM can classify a novel voxel as WM, GM, or CSF by reconstructing its tissue code. First, the intensities of a given voxel and its neighbours are used to set the activation of the nine corresponding nodes of the visible layer. Activation is then spread back and forth between the hidden and visible layers for two cycles, reconstructing the tissue code (see Figure 4). Finally, the voxel is classified as WM or CSF if those digits of the code are above a threshold (these thresholds are specific to each implementation of the CRBMseg algorithm); if neither the WM or CSF digits are above threshold, the voxel is classified as GM.

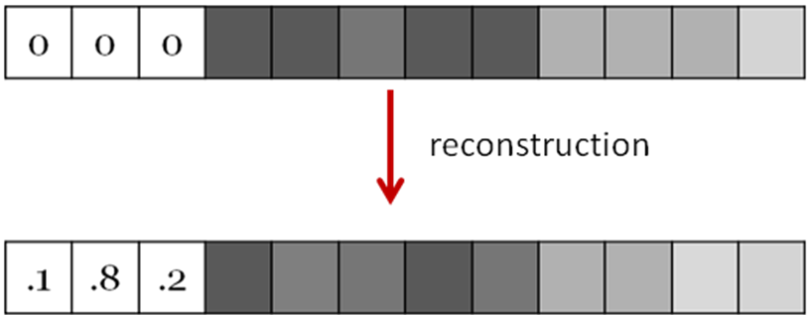

Figure 4. Tissue code reconstruction for a novel voxel.

CRBMs have several features which make them an appealing choice for use in an MRI segmentation algorithm over other alternatives (such as Markov random fields, or Gaussian probability models). Firstly, provided that the training dataset is representative of the population of test cases, a CRBM can perform well with a relatively limited number of training cases. Furthermore, because each node in a layer acts independently of the other nodes in that layer, the spread of activation through a CRBM network is highly parallelizable, and so can be implemented to take advantage of speedups provided by parallel computing hardware such as multicore processors and GPUs. Finally, unlike other segmentation algorithms which require an additional probability map for tissue types, once a CRBM has been trained it contains all of the information present in the training vectors implicitly.

CRBM Tissue Segmentation Pilot Implementation

A publicly available dataset of ground-truth expert brain MRI segmentations in NIFTI format is unfortunately not available. As such, the performance of the entire CRBMseg pipeline could not be evaluated within the timeline of this project. A pilot evaluation of the performance of the CRBM used in the pipeline, however, was conducted using brain MRI scan slices converted to 24bit PNG format.

Architecture

The CRBM used in the pilot implementation had 1000 nodes in the hidden layer (plus one bias node), and 12 visible layer nodes (plus one bias node). The 12 visible layer nodes accommodated the 12 dimensions of the input vectors. Specific model training parameters are listed in Table 1, and were estimated based on a guide provided by Geoffrey Hinton (2010). For tissue segmentation, a digit activation threshold of 0.5 was used for WM classification, and a threshold of 0.58 for CSF classification.

Table 1

Specific CRBM Parameters

Number of Hidden Units	1000
Learning Rate of Weights	0.65
Learning Rate of Sigmoid Function	0.50
Learning Cost	0.0001
Learning Momentum	0.80
Variance of Hidden Unit Activation	0.04

Training

The training data set was made up of 23245 input vectors from one half of one axial slice of a brain MRI volume alongside its naïve manual tissue segmentation map. The dimensions of the training slice were 120 by 285; there were 11138 WM training cases, 9207 GM cases, 2900 CSF cases, and 10955 pixels that did not include any of the three relevant tissues which were excluded from the set of training cases. The pilot CRBM was trained until it reached the specified error threshold of 0.001, which took 123 training epochs and 3 hours (Figure 5).

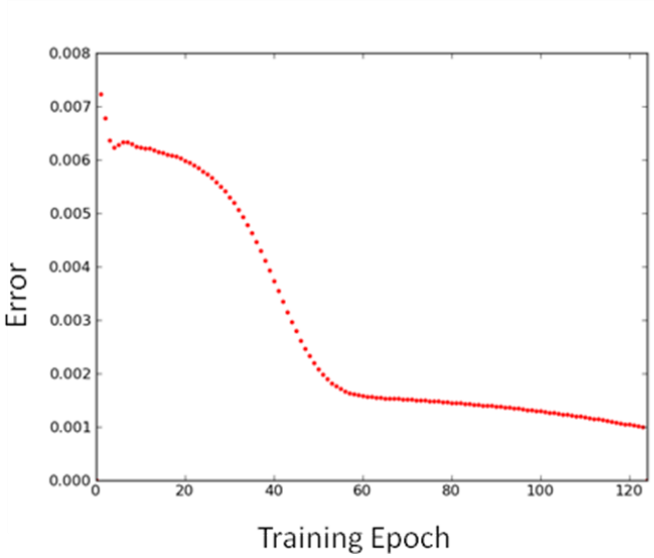

Figure 5. CRBM error over training epochs.

Testing with Novel Slices

Presented below in Figure 6 and Figure 7 are the CRBM's tissue segmentations of two novel skull-stripped MRI slices from the same volume as the training data. It is important to note that the training data only encompassed cerebral structures, so the CRBM is naively applying cerebral tissue segmentation patterns to subcortical structures.

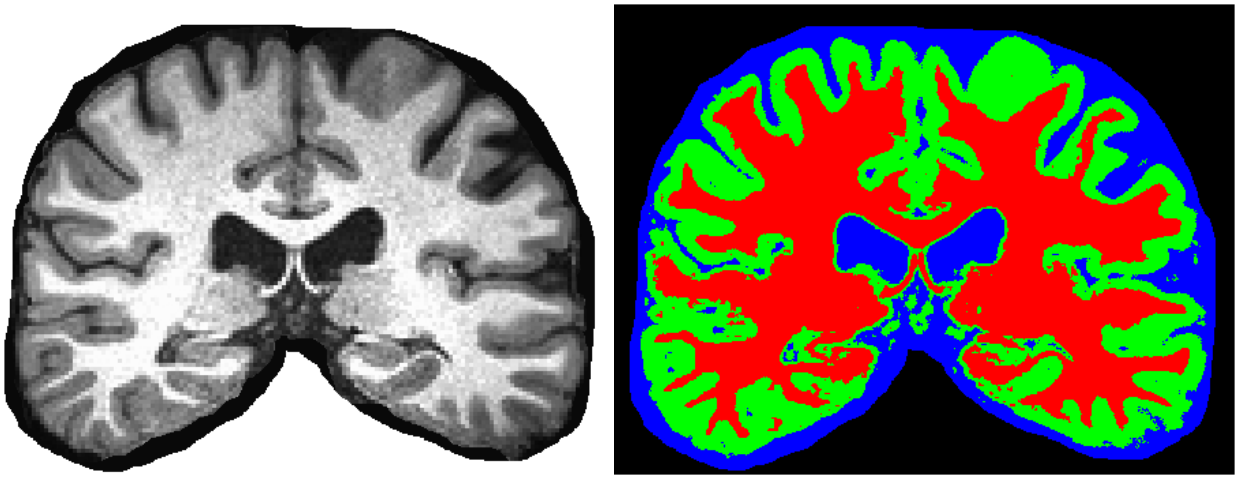

Figure 6. CRBM segmentation of a novel coronal MRI slice.

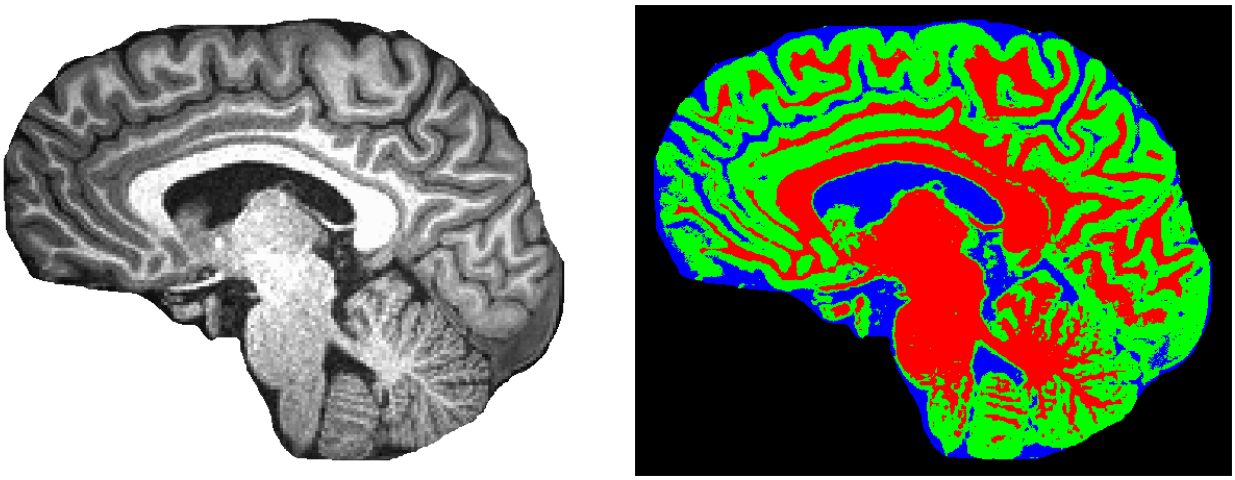

Figure 7. CRBM segmentation of a novel sagittal MRI slice.

Performance Evaluation

To evaluate the performance of the pilot implementation of the CRBM, I compared its segmentation performance to the other half of the axial slice used in training which was manually segmented in a similar fashion to the training dataset. Those results are presented in Figure 8 below.

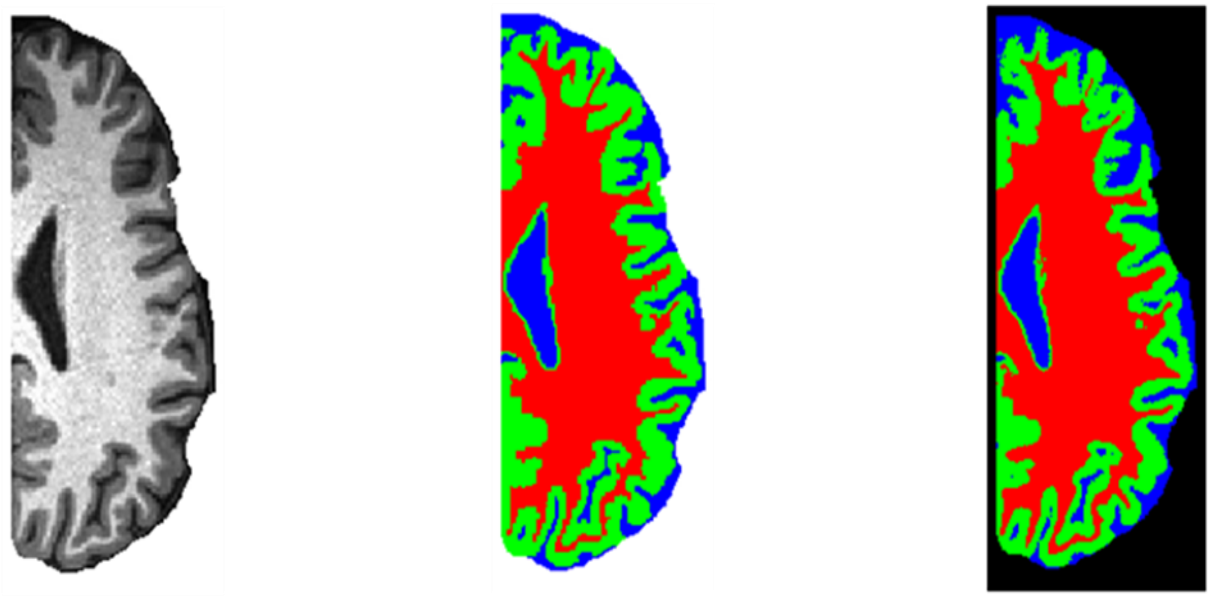

Figure 8. Comparison of segmentation results for a novel axial MRI slice.

The Dice coefficient between the manual segmentation and the CRBM segmentation was 0.91, and the Jaccard index was 0.84. These results are on par with the performance of the FAST algorithm and the SPM5-segment algorithm, which have been shown to have misclassification rates of approximately 10% (Tsang et al., 2008). Although this pilot implementation of the CRBM segmentation module is intended to serve solely as a proof of concept, these results suggest that the CRBMseg pipeline can approach and possibly surpass the performance of existing brain MRI tissue segmentation algorithms.

Future Directions

Aside from the obvious need to acquire a representative ground-truth dataset of manually segmented NIFTI brain MRI scans, there are two major improvements which can be made to the CRBMseg algorithm.

Firstly, improvements can be made in the implementation of the CRBM segmentation module. Although training and segmentation times at present are tractable (the automated segmentation of one slice takes less than one minute), the module's performance could be improved by implementing the large array operations which underlie the spread of activation from one layer to another in parallel on GPU. It is possible that even if CRBMseg is unable to outperform algorithms like SPM5-segment and FIRST in segmentation accuracy, with a parallel implementation it could significantly outperform them in terms of computation time.

Secondly, with NIFTI brain MRI volumes registered to a standard space (e.g. MNI 1mm), the three-dimensional coordinates of voxels could be integrated into the input vectors used for training and segmentation. Based on presumed anatomical commonalities between subjects, this would provide an implicit probabilistic map of areas where WM, GM, and CSF are most likely to be found. Implementing this improvement would require little change to the CRBM segmentation module; it would necessitate only the addition of three visible layer nodes and a method to read the coordinates of a given voxel into the input vector.

With these improvements to the CRBM segmentation module, alongside a representative dataset for training, the CRBMseg algorithm has a strong potential to equal or possibly outperform current state of the art brain MRI segmentation algorithms.

References

Ashburner, J., Friston, K. J., Poline, J., et al. (1995). Spatial registration and normalization of images. *Human Brain Mapping*, 2, 165– 189.

Carreira-Perpinan, M. A., & Hinton, G. E. (2004). On contrastive divergence learning. Retrieved from http://learning.cs.toronto.edu/~hinton/absps/cdmiguel.pdf

Chung, G., Dinov, I. D., Toga, A. W., & Vese, L. A. (2010). MRI tissue segmentation using a variational multilayer approach. In K. Miller & P. Nielsen (Eds.), *Computational Biomechanics for medicine,* doi: 10.1007/978-1-4419-5874-7_2 York: Psychology Press.

Gorgolewski, K., Burns, C. D., Madison, C., Clark, D., Halchenko, Y. O., Waskom, M. L., & Ghosh, S. S. (2011). Nipype: A flexible, lightweight and extensible neuroimaging data processing framework in python. *Frontiers in Neuroinformatics*, *5*(13), doi: 10.3389/fninf.2011.00013

Hinton, G. E. (2010). A Practical guide to training restricted Boltzmann machines. Retrieved from http://www.cs.toronto.edu/~hinton/absps/guideTR.pdf

Hinton, G. E., & Salakhutdinov, R. R. (2006). Reducing the dimensionality of data with neural networks. *Science, 303,* 504-507. Retrieved from http://www.cs.toronto.edu/~hinton/science.pdf

imonad.com. (2013). http://imonad.com/rbm/restricted-boltzmann-machine/

Mohamed, A. R., Hinton, G. (2010). Phone recognition using restricted Boltzmann machines. *IEEE International Conference on Acoustics Speech and Signal Processing*, 4354-4357, doi: 10.1109/ICASSP.2010.5495651

Patenaude, B., Smith, S., Kennedy, D., Jenkinson, M. (2007). Bayesian statistical models of shape and appearance for subcortical brain segmentation. *FMRIB Technical Report TR07BP1*, 1–23.

Smith, S. M., Jenkinson, M., Woolrich, M. W., Beckmann, C. F., Behrens, T. E. J., Johansen-Berg, H., Bannister, P. R., De Luca, M., Drobnjak, I., Flitney, D.E., Niazy, R., Saunders, J., Vickers, J., Zhang, Y., De Stefano, N., Brady, J.M., Matthews, P.M. (2004). Advances in functional and structural MR image analysis and implementation as FSL. *NeuroImage*, 23(S1), 208-219.

Tsang, O., Gholipour, A., Kehtarnavaz, N., Gopinath, K., Briggs, R., & Panahi, I. (2008). Comparison of tissue segmentation algorithms in neuroimage analysis software tools. *IEEE EMBS Conference*, doi: 978-1-4244-1815-2

Zhang, Y., Brady, M., Smith, S. (2001). Segmentation of brain MR images through a hidden Markov random field model and the expectation-maximization algorithm. *IEEE*

Transactions on Image Processing, 20(1), 45–57.